

# Volumetric Reconstruction from a Limited Number of Digitally Reconstructed Radiographs Using CNNs

Franz Thaler<sup>1,\*</sup>, Christian Payer<sup>1</sup> and Darko Štern<sup>2</sup>

**Abstract**— We propose a method for 3D computed tomography (CT) image reconstruction from 3D digitally reconstructed radiographs (DRR). The 3D DRR images are generated from 2D projection images of the 3D CT image from different angles and used to train a convolutional neural network (CNN). Evaluating with a different number of input DRR images, we compare our resulting 3D CT reconstruction to those of the filtered backprojection (FBP), which represents the standard method for CT image reconstruction. The evaluation shows that our CNN based method is able to decrease the number of projection images necessary to reconstruct the original image without a significant reduction in image quality. This indicates the potential for accurate 3D reconstruction from a lower number of projection images leading to a reduced amount of ionizing radiation exposure during CT image acquisition.

## I. INTRODUCTION

Aiming to visualize the interior body structure, computed tomography (CT) is not an invasive medical imaging technique, although it utilizes X-rays and as such, exposes the patient to radiation. Nevertheless, CT remains the dominant technique in three dimensional (3D) medical imaging due to fast acquisition and good quality of results. To visualize the interior structure of a subject, a 3D CT image is generated from a set of two dimensional (2D) X-ray images taken from different axial angles around the subject. A widely used method for 3D CT reconstruction from a set of 2D X-ray images is the filtered backprojection (FBP). By taking into account the angle from which the 2D X-ray images were acquired, FBP accumulates the backprojections of the filtered 2D X-ray images onto a 3D volume. A downside of the FBP method is that it requires a relatively high number of projections to give a reliable reconstruction, which directly correlates to the amount of radiation. Exposure to radiation increases the probability of cancer [11], which is especially problematic for applications dependent on frequent or repeated X-ray based imaging techniques.

Reducing the amount of radiation when generating 2D X-ray images lowers their quality and consequently also decreases the quality of the reconstructed 3D CT image. Different methods have been proposed to improve the quality of the reconstruction of a 3D CT image that is generated with low-dose radiation. In the approach [9] for improving the reconstruction quality, the low-dose CT sinogram data

restoration is combined with an advanced edge-preserving filter in the image domain. Due to latest achievements in machine learning approaches especially with convolutional neural networks (CNN) that outperformed humans in a classification task [2], deep neural networks became also attractive for reconstruction applications. In the low-dose CNN based reconstruction method proposed in [16], the quality of the X-ray image is increased by learning to improve each low-dose ray of the image. The method [5] applies a CNN to the wavelet transform coefficients to suppress noise that is specific to low-dose CT image acquisition.

Another group of methods that reduces radiation exposure are based on beam blockers, which partially block X-rays allowing only a subset of them to reach the subject's body. The works in [1] and [8] make use of a stationary blocker for scatter suppression using a compressed sensing technique. An evaluation in respect to the number of slits and the reciprocation frequency using moving beam blockers was done in [7]. In [12] low-resolution detectors are combined with high-resolution coded apertures to achieve super-resolution. The work of [17] applied a single-slice and a multi-slice super-resolution method on low-dose CTs to improve the image quality by utilizing a CNN. Differently from the blocker based methods, where the same number of X-ray projections is used, the same amount of radiation can be reduced without blocking the X-ray bins but decreasing the number of X-ray images used in the reconstruction of the CT image. However, these few-view CT images are heavily burdened by artifacts when FBP is used for reconstruction. The work of [3] proposed a gradient-based dictionary learning algorithm for CT reconstruction from a reduced number of views, using the vertical and horizontal gradient images as input. In the approach [18] a CNN is used to improve the quality of a few-view reconstructed images by learning its mapping to a full-view reconstruction.

An extreme case of CT reconstruction from a low number of X-ray images can also be found in 3D/2D image registration. As explained in [10] one approach for 3D/2D reconstruction is the intensity-based approach that aims to reconstruct the inter-operative 3D CT image from as few as possible X-ray images from different views. Namely, during minimally invasive surgeries it is required to exactly locate the instruments in use within the patient's body. To accomplish this, a high quality 3D CT image of a patient is acquired pre-operatively and registered with a single or multiple X-ray images from different directions that are generated inter-operatively. This is done repeatedly during surgery, exposing not only the patient but also the medical

\*This work was supported by the Austrian Science Fund (FWF): P28078-N33.

<sup>1</sup>Franz Thaler and Christian Payer are with the Institute of Computer Graphics and Vision, Graz University of Technology, Austria [f.thaler@student.tugraz.at](mailto:f.thaler@student.tugraz.at)

<sup>2</sup>Darko Štern is with the Ludwig Boltzmann Institute for Clinical Forensic Imaging, Graz, Austria [darko.stern@cfi.lbg.ac.at](mailto:darko.stern@cfi.lbg.ac.at)

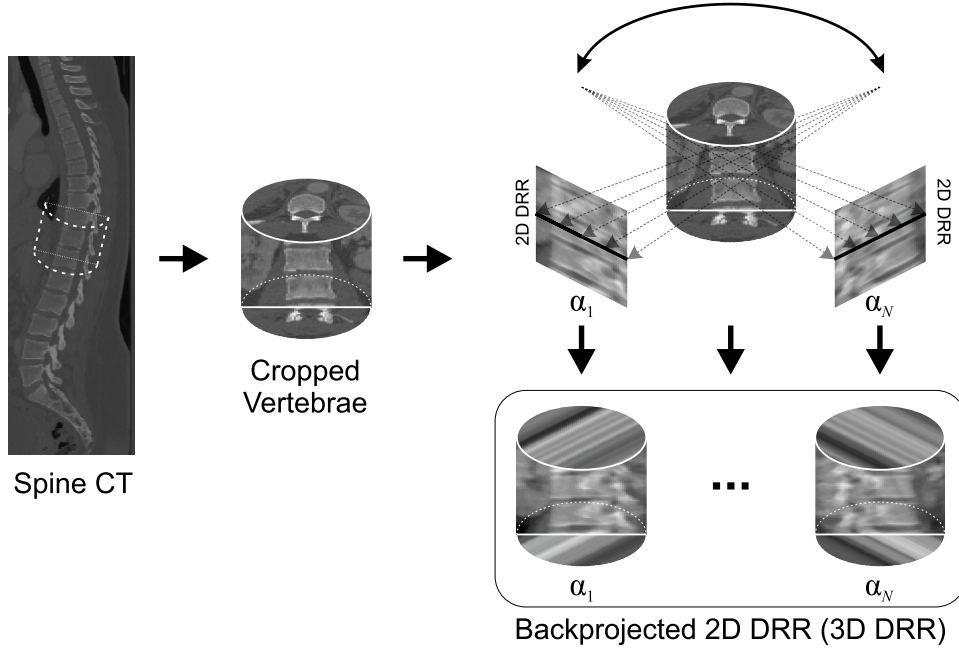


Fig. 1: Generation of digitally reconstructed radiographs (DRR) used in CNN based 3D reconstruction.

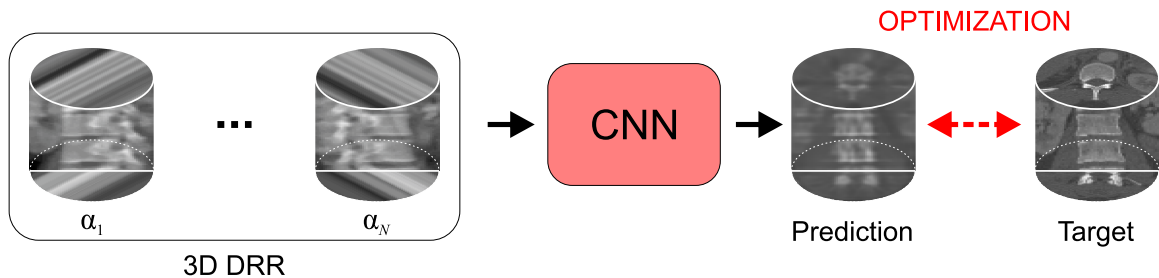


Fig. 2: Reconstruction of a 3D CT vertebra image from a limited number of backprojected 2D DRR images (3D DRR) using a U-Net based CNN.

staff to radiation.

A similar problem of reconstructing a 3D image given one or multiple 2D images is also seen in the computer vision community. The method in [14] utilizes a supervised learning approach to reconstruct depth information from a single RGB image. Resulting in a volumetric binary image, the method [15] based on a CNN uses a RGB image and depth information to recover a 3D shape of the scene. Multi-view reconstruction methods utilize multiple 2D input images from different views to reconstruct the surface of the scene in a 3D volumetric representation. For example the SurfaceNet introduced in [4] using a 3D CNN does not only use multiple images, but similar to CT reconstruction also the corresponding information of the angle from which each image is taken.

In this paper we propose a method based on a CNN for 3D CT image reconstruction from a limited number of 2D projection images. Our approach utilizes a framework that generates 2D digitally reconstructed radiographs (DRR) from an arbitrary direction and uses them to train a CNN for reconstructing the original 3D image. We conducted the

experiments with a different number of DRR images and compare the reconstruction results with the FBP method. We show that by using a machine learning based approach the number of images required for the reconstruction can be reduced without significant decrease in performance. The results indicate that our approach has a potential to be used for accurate 3D reconstruction from a lower number of views, thus reducing the amount of ionizing radiation.

## II. METHOD

In our method we generate 2D DRR images from different angles (Fig. 1) to be further used for training a CNN to reconstruct the original 3D CT image (Fig. 2). Due to their complex shape, which is challenging for reconstruction, we used spine images including several vertebrae for 3D CT reconstruction. These images are cropped from whole spine CT images and brought to the canonical position. DRR images are generated as a sum projection from the volumetric images in different angles. When generating DRR images the volumetric images are augmented by translation, rotation and scaling. Each generated DRR image is backprojected to a volume and used as input for training the U-Net based CNN

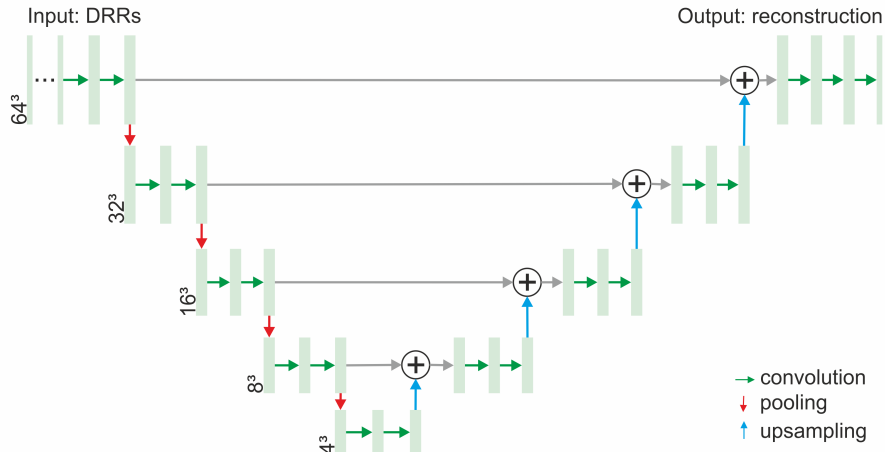


Fig. 3: Network architecture.

[13]. The reconstruction results of the CNN are quantitatively compared to the FBP approach.

The generation of the cropped 3D CT images of the vertebrae is explained in subsection II-A and the generation of DRR images in subsection II-B. Our network architecture is described in subsection II-C. A short overview of the FBP approach is presented in subsection II-D.

#### A. 3D CT Vertebra Image Generation

In our approach for 3D reconstruction from a reduced number of views, we used 3D CT images of vertebrae and their surrounding structure cropped from a whole spine CT as visualized in Fig. 1. Since each vertebra has a different orientation in the 3D spine image and to simplify the reconstruction task, we bring all vertebrae in the cropped 3D CT image to a canonical position, which is centered at the vertebral body's center, and defined by three orthogonal vectors representing the three dimensions. To find the position and orientation of the vertebra in the original spine image, we used two predefined points, i.e. a point in the center of the vertebra and at the tip of the spinous process. The first vector of the vertebra's orientation corresponds to the tangent vector of the polynomial curve connecting the centers of the vertebral bodies. The second vector corresponds to the direction of the spinous process' tip and the third vector is defined by the right hand rule. Based on the position and the orientation of each vertebra in the spine image, we cropped a cube that captures the vertebra and its surrounding structures.

#### B. 2D DRR Image Generation

In our approach we used 2D DRR images generated for reconstructing the cropped 3D CT vertebra image as explained in the previous subsection. The DRR images are generated as a sum projection of the cropped 3D CT vertebra image from an angle lying on the mid-axial plane of the volumetric image as shown in Fig. 1. We experimented with a different number  $N$  of 2D DRR images uniformly

distributed with fixed angles around the axial plane. Since each projection image for angle  $\alpha_n$ ,  $n = 1, \dots, N$  is identical to the projection image for angle  $\alpha_n + 180^\circ$ , we only generate DRR images from angles in the range of  $0^\circ$  to  $180^\circ$ .

#### C. Network Architecture

Our network architecture is based on the U-Net introduced in [13] and visualized in Fig. 3. Our CNN with volumetric kernels has a set of  $N$  3D DRR images as an input (Fig. 2). Each 3D DRR image corresponds to a single 2D DRR image backprojected to a volume of the same size as the original 3D vertebra image (Fig. 1). A 3D DRR image is created by repeating the 2D DRR image in the volume shifted by the angle  $\alpha_n$  that corresponds to the direction the 2D DRR image was acquired from.

Our CNN architecture is defined as follows: for each level in the contracting path, two consecutive convolution layers are used while a subsequent average pooling layer creates the input for the next lower level. When the maximum number of levels is reached, the two convolutions are followed by an upsampling layer. This upsampling layer is then merged with the convolution layer output of the contracting path of the same level by utilizing an add layer. In the expanding path, every upsampling and add layer is followed by two convolution layers until the original size of the image is reached. After that, a final convolution with output size one generates the prediction corresponding in size to the 3D vertebra image. To obtain the CNN parameters  $\omega$  we used  $L_1$  loss between all voxels  $m \in M$  of the predicted image  $\hat{p}$  and the 3D vertebra image  $p$ :

$$\hat{\omega} = \arg \min_{\omega} \frac{1}{m} \sum_{m \in M} |\hat{p}_m(\omega) - p_m|. \quad (1)$$

#### D. Filtered Backprojection

We compare our results with the standard approach used in CT reconstruction, represented by the FBP. Since simply summing up the backprojected 2D DRR images, i.e. the 3D DRR images, gives a blurry reconstruction of the original

3D image, the FBP utilizes a ramp filter  $R$  to reduce the contribution of low frequencies in Fourier space  $\mathcal{F}$  before summation. Thus, before doing backprojection, each ray of the 2D DRR images  $I_j \in I$  is transformed to the frequency domain by utilizing the Fourier transform and is multiplied with a ramp filter. After applying the inverse Fourier transform  $\mathcal{F}^{-1}$ , the filtered rays  $\hat{I}_j$  are returned to their original position in the 2D DRR image  $\hat{I}$ :

$$\hat{I}_j = \mathcal{F}^{-1}(R \cdot \mathcal{F}(I_j)). \quad (2)$$

### III. EVALUATION

#### A. Material

The data used in this work encompasses CT scans of the spine of 10 different patients from which we extracted all present vertebrae. The spine CTs vary in size, spacing and vertebrae contained within them. The volumes have a size of  $512 \times 512 \times K$ , where  $K$  ranges from 507 to 625. The number of vertebrae included in the volumes ranges from 17 to 19, giving us a total of 176 vertebrae. We separated the CT images into a training and a test set in the ratio of 80 to 20, i.e. we used eight spines for training and two spines for testing. As a result, the training set encompasses 141 vertebrae and the test set 35.

As a first step, all 3D CT spine images are transformed to have an equal size. Since the spacing parameter takes care of the real world mapping, which keeps the image ratios intact, rescaling the 3D CT images does not lead to any distortion. Also, since the CT spine images have a high resolution for being 3D, we also downsample the spine images to  $256 \times 256 \times 256$ , which is approximately half the size in each dimension. The CT images are downsampled with tricubic interpolation and then stored to the hard drive and used for any further processing. By utilizing this downsampling, image loading is accelerated and the memory consumption is reduced.

#### B. Augmentation

For the CNN to be successfully trained, a training data set that consists of target 3D vertebra images and corresponding single- or multi-view input 3D DRR images has to be increased. Therefore, we utilized online augmentation, which performs a translation, rotation and scaling when cropping the 3D vertebra images from the original CT spine images. We performed a translation by dislocating the center of the vertebral body in all three dimensions and a rotation by adding an offset to the angle of each of the orthogonal vectors defining the canonical position of the vertebra. In contrast to translation and rotation, scaling is performed uniformly in all three dimension to prevent a distortion of anatomical structures. We did not argument the angle  $\alpha_n$  of the projection 2D DRR images.

#### C. Experimental Setup

Our hardware setup consisted of a CPU Intel Core i7-930 @ 2.80GHz, 24 GB RAM and a GeForce GTX TITAN X

with 12 GB. We implemented our network in Keras<sup>1</sup> using TensorFlow<sup>2</sup> as it's backend, volumetric image processing was done utilizing the ITK framework<sup>3</sup>.

The target 3D vertebra images we used as ground truth have a size of  $64 \times 64 \times 64$  voxels and their size in physical space is set to 120 mm per dimension. For online 3D vertebra image augmentation we set the translation range to 15 mm, the rotation range to  $30^\circ$  and the scaling percentage to 15%. We utilized a uniform distribution to generate the augmentation parameters and the order of execution is rotation, translation and scaling.

Due to the different amount of image information projected from different angles when generating the 2D DRR images from the 3D vertebra image cropped as a cube, we introduced the same cylindrical mask to all the 3D cropped vertebra images before generating 2D DRR images. Additionally, when calculating the loss function in Eq. (1), only the pixels  $M$  inside the cylinder are taken into account.

For the implementation of the FBP we utilized the open source library scikit-image<sup>4</sup> on our data.

We trained our network with a mini-batch size of one for 200 epochs, each of them used 200 iterations, resulting in a total of 40.000 samples used for training. As a loss function we utilized  $L_1$  given in Eq. (1), a weight regularization was done with  $L_2$  and a factor of 0.0005. As an optimizer we used Adam [6], the learning rate was set to 0.0002, the first and second moment estimates are defined as  $\beta_1 = 0.9$  and  $\beta_2 = 0.999$ . All convolution layers are defined as volumetric convolutions, we used zero padding and as kernel initializer we utilized He normal [2]. For all convolutions except the final one, we used a kernel size of  $3 \times 3 \times 3$ , 64 filters and ReLU as activation function. The final convolution's kernel size was set to  $1 \times 1 \times 1$ , we used just one filter and no activation function. Furthermore, we used 3D average pooling and 3D nearest neighbor upsampling layers with a kernel size of  $2 \times 2 \times 2$ .

### IV. RESULTS

We train individual networks for different numbers  $N$  of 3D DRR input images and compare the predicted 3D reconstruction quantitatively and qualitatively to the results of the FBP. Fig. 4 and Table I show the mean absolute error to the target 3D vertebra images used as ground truth for both methods respectively. The center slice of the ground truth of one 3D vertebra image as well as our qualitative results and those from the FBP are presented in Fig. 5 and 6. All images represent the reconstruction of the same 3D vertebra image using a different number of views,  $N \in \{1, 2, 3, \dots, 120, 180\}$ . All vertebra image slices included in our qualitative results correspond to one another by having the exact same center voxel. Furthermore, the brightness setting is identical for all vertebra image slices, however, for better contrast some values are truncated. This is especially true for the FBP

<sup>1</sup><https://keras.io/>

<sup>2</sup><https://www.tensorflow.org/>

<sup>3</sup><https://itk.org/>

<sup>4</sup><http://scikit-image.org/>

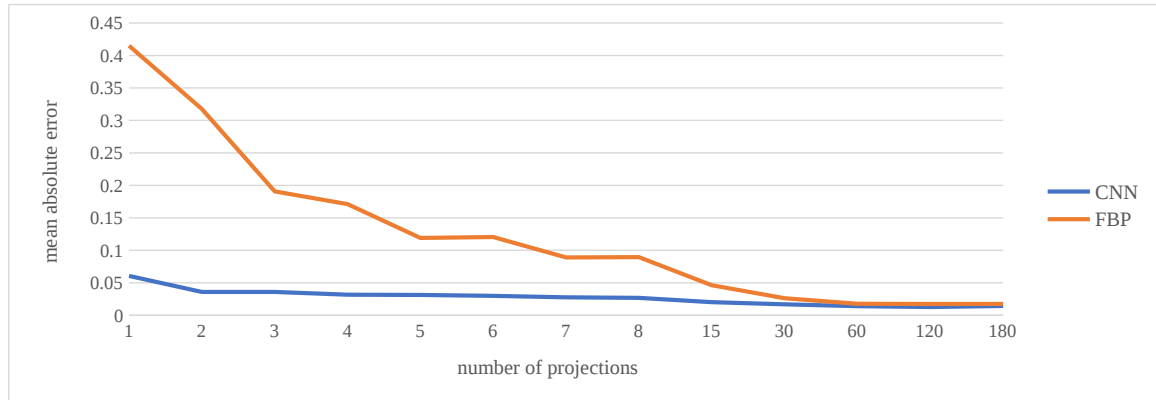


Fig. 4: Mean absolute error of our CNN and FBP to ground truth for a different number of projection images ( $N$ ).

results using only very few views, since they show a large deviation in color value.

TABLE I: Mean absolute error  $\pm$  standard deviation of our CNN and FBP to ground truth.

Projections ( $N$ )	CNN ( $10^{-2}$ )	FBP ( $10^{-2}$ )
1	6.06 $\pm$ 2.24	41.50 $\pm$ 7.39
2	3.59 $\pm$ 0.80	31.77 $\pm$ 5.43
3	3.59 $\pm$ 0.72	19.07 $\pm$ 3.32
4	3.17 $\pm$ 0.58	17.11 $\pm$ 2.87
5	3.12 $\pm$ 0.58	11.90 $\pm$ 1.88
6	2.99 $\pm$ 0.63	12.04 $\pm$ 2.07
7	2.76 $\pm$ 0.51	8.90 $\pm$ 1.43
8	2.68 $\pm$ 0.53	8.95 $\pm$ 1.46
15	2.02 $\pm$ 0.38	4.63 $\pm$ 0.73
30	1.69 $\pm$ 0.33	2.62 $\pm$ 0.37
60	1.40 $\pm$ 0.26	1.76 $\pm$ 0.23
120	1.27 $\pm$ 0.21	1.74 $\pm$ 0.23
180	1.43 $\pm$ 0.30	1.74 $\pm$ 0.23

## V. DISCUSSION

To visualize the interior body structure CT imaging utilizes a number of X-ray images captured from different axial angles. Involving a large number of X-ray images increases the ionizing radiation not only to the patient but also to the medical staff involved in the image acquisition. Reducing the number of views from which X-ray images are generated leads to a significant decrease in the quality of the 3D CT image, when reconstructing with the standard FBP method. In this work we investigate the potential of a machine learning based approach to improve the quality of the reconstructed images when the number of views is limited. Inspired by the previous work in [4] that comes from the computer vision community, we constructed a framework that reconstructs the volumetric image based on multi-view 2D images. Compared to [4] that use camera images with a higher number of views to reconstruct the surface of an outdoor scene, in our approach the 3D CT image is reconstructed from a sparse number of 2D projection images. Differently from [16], where high quality single axial CT reconstruction was done from the low quality 2D image obtained by accumulating few-view backprojections, our

CNN based method reconstructs the 3D CT image directly from the backprojected DRR images.

When utilizing deep CNNs, a significant number of training data is required, which in our scenario of CT reconstruction would require access to a large set of X-ray projection images used for CT reconstruction. Therefore, in this paper we investigate the possibility of using DRR images as a substitution for the real X-ray images, thus, showing that CNNs combined with 2D DRR images can be used for reconstructing 3D CT images. We followed the standard backprojection procedure used in CT reconstruction but replaced the backprojection of the X-ray images with the backprojected DRR images, i.e. 3D DRR images. CNNs are then trained to compensate the missing information coming from omitted backprojected X-ray images.

The quantitative results in Fig. 4 and Table I show that our method performs better than the FBP for a small number of views and almost the same when a large number of DRR images is used. Thus, the quality of the 3D reconstruction becomes almost the same for both methods when using 60 3D DRR images as input. However, as seen in Fig. 5 and 6, when using 30 3D DRR images from different angles our method already provides good qualitative results with only a small amount of artifacts present in the 3D CT reconstruction, whereas the FBP still suffers from a lot of artifacts. Moreover, our method is able to visualize all important structures of the vertebra in the reconstruction of the 3D image by utilizing only 15 different views. Using only two 3D DRR images, the silhouette of the vertebra reconstructed by our method can be recognized especially in sagittal view, while the FBP method requires eight views for a similar quality of the reconstructed images. For a single 3D DRR input image, neither our nor the FBP method managed to produce useful results.

By showing a better quality than the FBP method when using a small number of DRR images to reconstruct a 3D CT image, the results indicate that our method can be used to reduce the number of X-ray images to reconstruct 3D CT images in real world scenarios. Thus, our method shows that by utilizing a CNN it is possible to reduce the overall amount of radiation during 3D reconstruction. Reducing the exposure

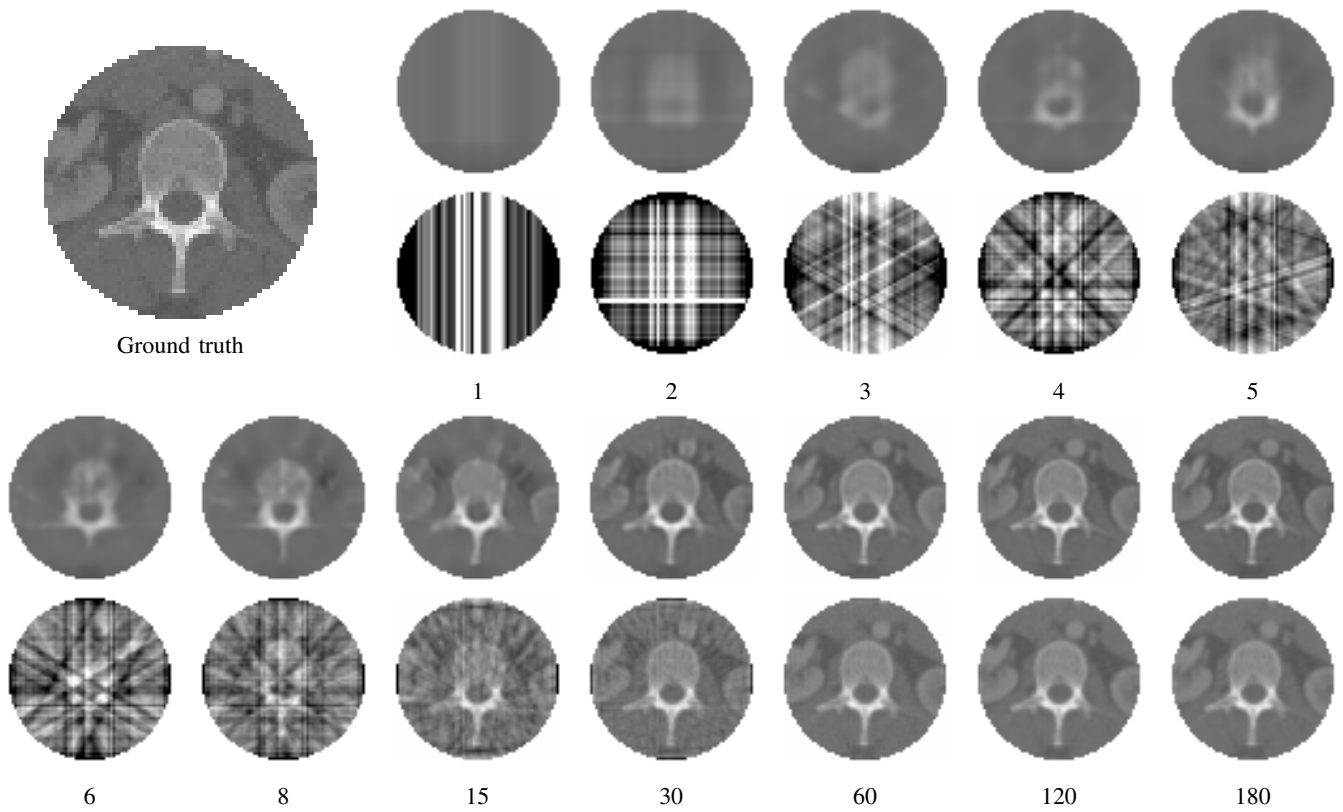


Fig. 5: Qualitative results of axial slices for different number of projection views comparing our method (top images) with FBP (bottom images). Ground truth is shown on top left.

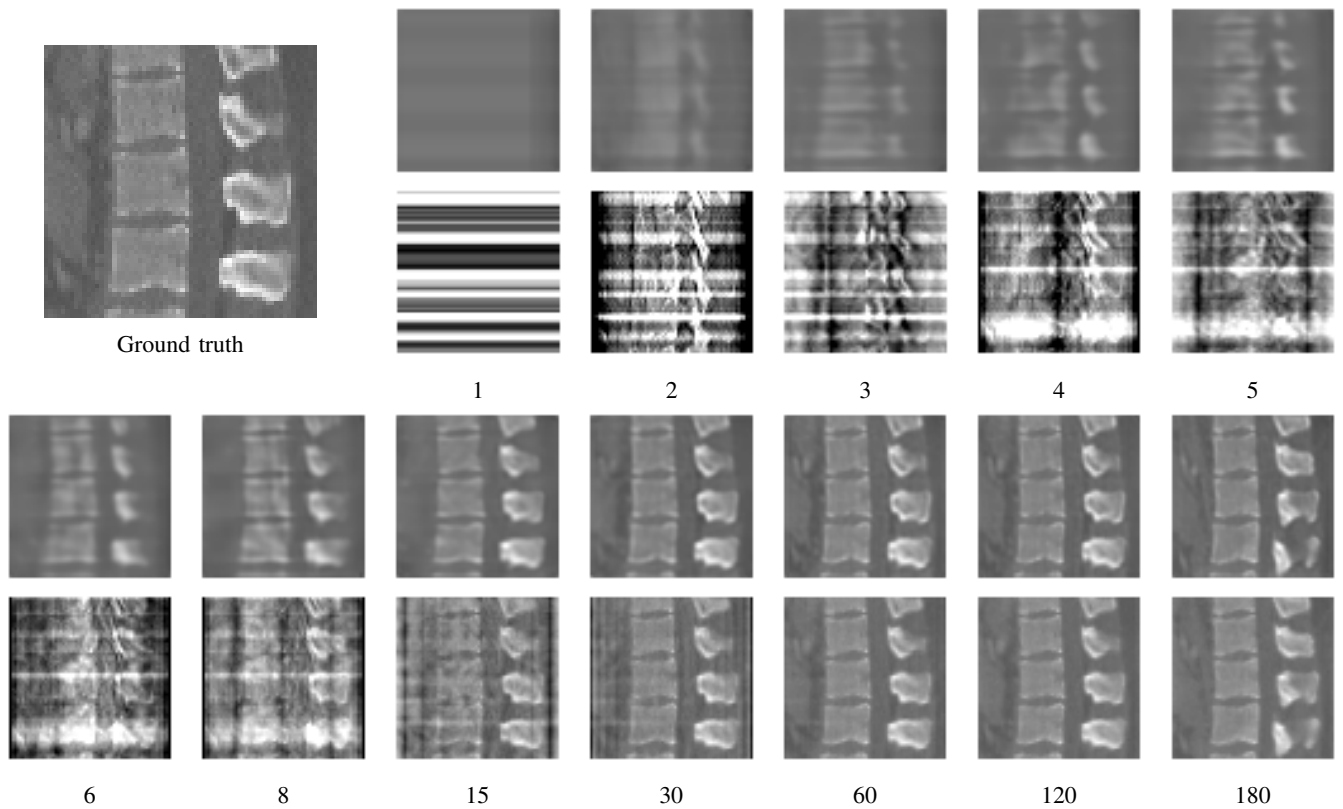


Fig. 6: Qualitative results of sagittal slices for different number of projection views comparing our method (top images) with FBP (bottom images). Ground truth is shown on top left.

to ionizing radiation for patients during CT image acquisition is especially beneficial when patients are subject to frequent examinations. Another beneficial application of our method could be for a scenario, when it is unfavorable or not feasible to acquire a large amount of views. An example of such a case is 3D/2D registration during minimally invasive and image guided surgeries, where 3D reconstruction from a limited number of X-ray images decreases the exposure of both patients and medical staff to ionizing radiation.

## VI. CONCLUSION

In this paper we proposed a method for multi-view 3D CT image reconstruction from 3D DRR images using machine learning. Our method improves the quality of the reconstructed 3D CT image compared to the standard FBP by utilizing a CNN for a small number of views and gives similar results for a high number of views. By reducing the number of 3D DRR images required for a 3D CT reconstruction, our method indicates the possibility to decrease the amount of necessary X-ray images in real world scenarios. Thus, it is possible to reduce the amount of ionizing radiation exposed to the patient and the medical staff during image acquisition for examination and surgery. In our future work, we aim to further improve the quality of the results as well as to evaluate the performance of our approach on different datasets.

## REFERENCES

- [1] X. Dong, M. Petrongolo, T. Niu, and L. Zhu, "Low-dose and scatter-free cone-beam CT imaging using a stationary beam blocker in a single scan: phantom studies," *Computational and mathematical methods in medicine*, vol. 2013, 2013.
- [2] K. He, X. Zhang, S. Ren, and J. Sun, "Delving deep into rectifiers: Surpassing human-level performance on imagenet classification," in *Proceedings of the IEEE international conference on computer vision*, 2015, pp. 1026–1034.
- [3] Z. Hu, Q. Liu, N. Zhang, Y. Zhang, X. Peng, P. Z. Wu, H. Zheng, and D. Liang, "Image reconstruction from few-view CT data by gradient-domain dictionary learning," *Journal of X-ray science and technology*, vol. 24, no. 4, pp. 627–638, 2016.
- [4] M. Ji, J. Gall, H. Zheng, Y. Liu, and L. Fang, "Surfacenet: An end-to-end 3D neural network for multiview stereopsis," in *Proceedings of the IEEE Conference on Computer Vision and Pattern Recognition*, 2017, pp. 2307–2315.
- [5] E. Kang, J. Min, and J. C. Ye, "A deep convolutional neural network using directional wavelets for low-dose X-ray CT reconstruction," *Medical physics*, vol. 44, no. 10, 2017.
- [6] D. P. Kingma and J. Ba, "Adam: A method for stochastic optimization," *International Conference on Learning Representations 2015*, pp. 1–15, 2015.
- [7] T. Lee, C. Lee, J. Baek, and S. Cho, "Moving beam-blocker-based low-dose cone-beam CT," *IEEE Transactions on Nuclear Science*, vol. 63, no. 5, pp. 2540–2549, 2016.
- [8] W. Liu, J. Rong, P. Gao, Q. Liao, and H. Lu, "Algorithm for X-ray beam hardening and scatter correction in low-dose cone-beam CT: Phantom studies," in *Medical Imaging 2016: Physics of Medical Imaging*, vol. 9783. International Society for Optics and Photonics, 2016, p. 978332.
- [9] J. Ma, J. Huang, Z. Liang, H. Zhang, Y. Fan, Q. Feng, and W. Chen, "Image fusion for low-dose computed tomography reconstruction," in *Nuclear Science Symposium and Medical Imaging Conference (NSS/MIC)*, 2011 IEEE. IEEE, 2011, pp. 4239–4243.
- [10] P. Markelj, D. Tomaževič, B. Likar, and F. Pernuš, "A review of 3D/2D registration methods for image-guided interventions," *Medical image analysis*, vol. 16, no. 3, pp. 642–661, 2012.
- [11] D. L. Miglioretti, E. Johnson, A. Williams, R. T. Greenlee, S. Weinmann, L. I. Solberg, H. S. Feigelson, D. Roblin, M. J. Flynn, N. Vanneman, *et al.*, "The use of computed tomography in pediatrics and the associated radiation exposure and estimated cancer risk," *JAMA pediatrics*, vol. 167, no. 8, pp. 700–707, 2013.
- [12] E. Mojica, S. Pertuz, and H. Arguello, "High-resolution coded-aperture design for compressive X-ray tomography using low resolution detectors," *Optics Communications*, vol. 404, pp. 103–109, 2017.
- [13] O. Ronneberger, P. Fischer, and T. Brox, "U-Net: Convolutional networks for biomedical image segmentation," in *International Conference on Medical image computing and computer-assisted intervention*. Springer, 2015, pp. 234–241.
- [14] A. Saxena, S. H. Chung, and A. Y. Ng, "3-D depth reconstruction from a single still image," *International journal of computer vision*, vol. 76, no. 1, pp. 53–69, 2008.
- [15] Z. Wu, S. Song, A. Khosla, F. Yu, L. Zhang, X. Tang, and J. Xiao, "3D shapenets: A deep representation for volumetric shapes," in *Proceedings of the IEEE conference on computer vision and pattern recognition*, 2015, pp. 1912–1920.
- [16] X. Yang, V. De Andrade, W. Scullin, E. L. Dyer, N. Kasthuri, F. De Carlo, and D. Gürsoy, "Low-dose X-ray tomography through a deep convolutional neural network," *Scientific reports*, vol. 8, no. 1, p. 2575, 2018.
- [17] H. Yu, D. Liu, H. Shi, H. Yu, Z. Wang, X. Wang, B. Cross, M. Bramler, and T. S. Huang, "Computed tomography super-resolution using convolutional neural networks," in *Image Processing (ICIP), 2017 IEEE International Conference on*. IEEE, 2017, pp. 3944–3948.
- [18] J. Zhao, Z. Chen, L. Zhang, and X. Jin, "Few-view CT reconstruction method based on deep learning," in *Nuclear Science Symposium, Medical Imaging Conference and Room-Temperature Semiconductor Detector Workshop (NSS/MIC/RTSD)*, 2016. IEEE, 2016, pp. 1–4.